



Science Arts & Métiers (SAM)

is an open access repository that collects the work of Arts et Métiers Institute of Technology researchers and makes it freely available over the web where possible.

This is an author-deposited version published in: <https://sam.ensam.eu>
Handle ID: [.http://hdl.handle.net/10985/10243](http://hdl.handle.net/10985/10243)

To cite this version :

Mohamad YOUNES, Philippe DAL SANTO, Alain POTIRON - Three-dimensional study for the relative positioning of mechanical elements in mechanisms constituted by parrallel joints with clearances - Mechanical Engineering: An International Journal (MEIJ) - Vol. 1, n°1, p.1-22 - 2014

Any correspondence concerning this service should be sent to the repository

Administrator : scienceouverte@ensam.eu



THREE-DIMENSIONAL STUDY FOR THE RELATIVE POSITIONING OF MECHANICAL ELEMENTS IN MECHANISMS CONSTITUTED BY PARALLEL JOINTS WITH CLEARANCES

Mohamad Younes¹, Philippe Dal Santo², Alain. Potiron²

¹ Lebanese University, University Institute of Technology, Saida, Lebanon

² Ecole Nationale Supérieure d'Arts et Métiers, Laboratoire LAMPA Arts et Métiers Paris Tech Angers, 2 boulevard du Ronceray, BP 3525, 49035 Angers Cedex, France

ABSTRACT

The great evolution of the data-processing tools during the last years allowed for the development of the computer aided design in the field of mechanical structures. Controlling the clearance in joints between parts, is one of the required objectives to provide accurate relative movements and to minimize geometrical errors. For that purpose, a new method of static study allowing for the computation of the equilibrium positions of various elements in spatial mechanisms constituted by parallel joints and subjected to mechanical loadings is proposed. The isostatic study takes into account the presence of the clearance in the mechanism joints. The method is based to the minimization of the potential energy by means of some algorithms of optimization. The results obtained show the effectiveness of the method.

KEYWORDS

Mechanism Analysis, Joint Clearance, Optimization

1. INTRODUCTION

Between bodies assembly constituting a machine, clearance in the joints are necessary to ensure the relative movements of links. Unfortunately, it is that presence of clearance which causes mechanical vibrations, noise and inaccuracy in the relative movement of multi-links mechanism. Some numerical methods were developed in the C.A.D field in order to control the joints clearance and to minimize geometrical errors of position in the mechanism.

Nevertheless, it appears that a rather small number of researches were carried out in this field. The main part of the works concerning the computation of the relative positions of mechanism elements linked by joints with clearance, are carried out from a strict geometrical point of view.

Potiron et al. [1] proposed a new method of static analysis in order to determine the arrangement of the various components of planar mechanisms subjected to mechanical loadings. The study takes into account the presence of linkage clearance and allows for the computation of the small variations of the parts position compared to the large amplitude of the movements useful for the power transmission.

It appears that a rather small number of research tasks were carried out in this particular field. Funabashi et al. [2] tackled the problem by carrying out a dynamic, theoretical and experimental study of some simple mechanisms. In order to specify the influence of the clearance in the links on machine operations, they derived the equations of the movement of links including parts stiffnesses, viscous friction and Coulomb's friction in joints. The results are interesting for the specific models suggested but they don't lead to a general usable method suited for the study of complex mechanisms.

A model of mechanism with joint's clearance was defined by Giordano et al. [3] when researching the dimensional and geometrical tolerances associated with machine elements. The method is based on the definition of small rigid-body displacements and the use of closed loops equations for the associated kinematic chains.

With Giordano and Duret [4], they developed a mathematical model and give a geometrical interpretation of the gaps by defining a «hyperspace of gaps». By means of this «gap-space», it is possible to define the compatibility of the tolerances assigned to the manufactured parts. However, the study didn't take into account neither the geometrical defects of the parts nor the deformations and feature variations resulting from the applied loads.

To improve the quality of manufactured products and reduce their total cost, Gao et al. [5] and Chase et al. [6] have developed a method for the tolerance analysis of two and three-dimensional mechanical assemblies. This method is carried out by a direct linearization of a geometrical non-linear problem. It was implemented in a commercial C.A.D. code, in order to extract from the results, acceptable tolerances and the dimensions of the related parts.

In the same topic, Chase and Parkinson [7] presented an outline on recent research in the analysis of mechanical tolerances, from which it is possible to have an idea of how to handle the study of the joints' clearance in mechanisms.

Flores and Ambrosio [8] presented a computational methodology for dynamic analysis of multibody mechanical systems with joint clearance. The model for planar revolute joints is based on a thorough geometric description of contact conditions and on a continuous contact force model, which represents the impact forces. It is shown that the model proposed lead to realistic contact forces. These forces correlate well with the joint reaction forces of an ideal revolute joint, which correspond to a joint with zero clearance.

Turner et al. [9] proposed a methodology for constructing spherical four-bar mechanisms with an emphasis on utilizing simpler machining processes and part geometries. By building each link out of easily created pieces instead of a single complex shape, a mechanism can be quickly prototyped and tested.

Liu et al. [10] presented a method concerned with the determination of the normal force-displacement relation for the contact problem of cylindrical joints with clearance. A simple formulation for this contact problem is developed by modeling the pin as a rigid wedge and the elastic plate as a simple Winkler elastic foundation.

Thomas et al. [11] proposed a new notation for kinematic structures which allows a unified description of serial, parallel, and hybrid robots or articulated machine tools. They tried to fill this gap by presenting a new notation, which is based on the graph representation known from gear trains.

In the works of Fischer [12], the ball joint often referred to as a spherical or 'S' joint is modeled using dual-number coordinate-transformation matrices. The joint consists of concave and convex spherical surfaces engaged to prevent translations but allowing three degrees of freedom, all of which are rotations.

Hsieh [13] has proposed a method allowing for the kinematic description of mechanisms containing prismatic, revolute, helical and cylindrical joints to be explicitly defined, it cannot be directly applied to mechanical systems containing spherical pairs. Accordingly, he proposed an extended D-H notation which allows the independent parameters of any spatial mechanism, including one with spherical pairs, to be derived for analysis and synthesis purposes. The validity of the proposed notation is demonstrated via its application to the analysis of mechanisms containing revolute, spherical, cylindrical and prismatic joints.

In the study of Erkaya and Uzmay [14] a dynamic response of mechanism having revolute joints with clearance is investigated. A four-bar mechanism having two joints with clearance is considered as a model of mechanism. A neural network was used to model several characteristics of joint clearance. Kinematic and dynamic analyses were achieved using continuous contact mode between journal and bearing. A genetic algorithm was also used to determine the appropriate values of design variables for reducing the additional vibration effect due primarily to the joint clearance.

In this work, a general quasi-static method is proposed to determine the relative positions of mechanisms links with joints clearance.

Being given a geometrical position resulting from the great amplitude of movements in the parallel mechanism, it will be possible to compute the equilibrium positions of the various parts by taking into account the clearance in the linkages. The main idea is to define and minimize an objective function which, in the present case, is the potential energy of the mechanism. This is carried out by taking account of the geometrical constraints imposed by the clearance on infinitely small displacements in the joints.

During these studies, several simplifying assumptions will be formulated:

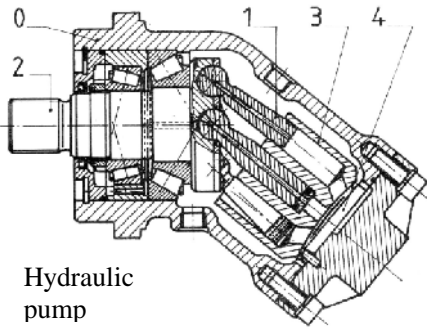
- the joints in the mechanism are carried out with clearances,
- the solids are not deformable,
- the solids are geometrically perfect, i.e. the shape defects due to machining tolerances are ignored,
- the gravity force is neglected compared to others applied forces.

2. MECHANISM MODELING ASSUMPTIONS

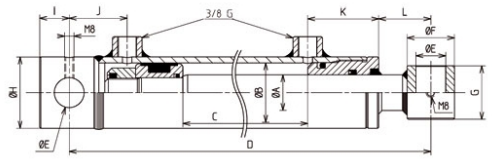
2.1. Examples of real mechanisms

In various mechanical devices such as pumps, hydraulic motors, hydraulic tubes, etc. each component is linked to others by means of different joints (spherical, cylindrical, prismatic, etc.). In each of them there exists some clearance which can perturb the movements or (and) reduces the relative position accuracy between the links.

Some mechanisms are represented in the following figures which exhibit several components linked together with some common joints.



Hydraulic pump



Hydraulic tube

Pump housing (0), plunger (1), shaft (2), cylinder barrel (3), hydraulic distributor (4)

Figure 1. Two mechanical devices with common joints

2.2. Clearance space modeling

In Figure 1 above, it is supposed that some clearance with values J_i exists in the different joints. In the study, the real parts are associated with a joint space. Each part is replaced by lines without transverse dimensions and the joint is replaced by a geometrical space with dimensions equal to clearance. The distances between joints on the same part are conserved. An example is given in Figure 2 below.

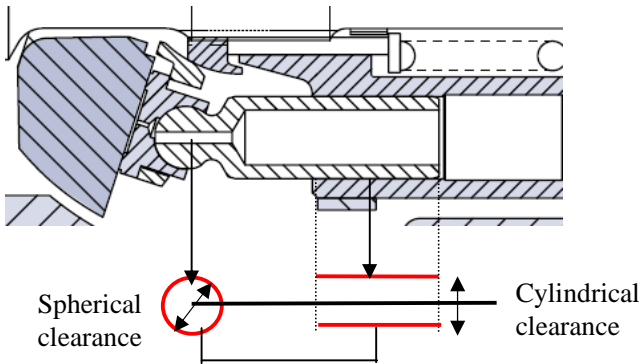


Figure 2. Clearance modeling

The sketch in Figure 2 and the others presented in the following expand the joint clearance compared to the other dimensions of the mechanism and they do not take into account the scale of the figure.

3. BASIC THEORY FOR THE MECHANISM WITH PARALLEL JOINTS

3.1. Rigid-body small displacements

The mechanism is composed of two parts S_1 and S_0 linked together by two joints l_1 and l_2 . The points A_1 and A_2 appearing in equation (1), lie on the center line of the link. They coincide respectively with the two points O_1 and O_2 "centers" of the joints l_1 and l_2 in the initial position.

OXYZ is the global reference frame with its origin O. $O_1X_1Y_1Z_1$ and $O_2X_2Y_2Z_2$ are the local reference frames of the joints with origins O_1 and O_2 . O_1 is currently chosen to coincide with O.

In the absence of great amplitude movements, the relative motion of a body S_1 compared to a body S_0 in the center A_i ($i=1,2$) of the joint l_i is represented by the following kinematic vectorial-set $\{\mathcal{T}_i(S_1/S_0)\}$:

$$\{\mathcal{T}_i(S_1/S_0)\} = \{\Omega_i(S_1/S_0), \mathbf{V}_{A_i}(S_1/S_0)\}_{A_i} \quad (1)$$

$\Omega_i(S_1/S_0)$ and $\mathbf{V}_{A_i}(S_1/S_0)$ are respectively the rotation vector and the displacement vector of S_1 at point A_i of S_1 relative to the origin O_i of the joint l_i . In the case of three-dimensional study, $\Omega_i(S_1/S_0)$ and $\mathbf{V}_{A_i}(S_1/S_0)$ are written in the form of:

$$\Omega_i(S_1/S_0) = \begin{Bmatrix} \alpha_i \\ \beta_i \\ \gamma_i \end{Bmatrix} \quad (2.a) \quad \text{and} \quad \mathbf{V}_{A_i}(S_1/S_0) = \begin{Bmatrix} u_i \\ v_i \\ w_i \end{Bmatrix} \quad (2.b)$$

The unknowns parameters of the problem are the components u_i , v_i , w_i , α_i , β_i , et γ_i , of the two vectors $\Omega_i(S_1/S_0)$ and $\mathbf{V}_{A_i}(S_1/S_0)$.

Remark

In the following, for infinitely small rotation θ_i , $\sin \theta_i \approx \tan \theta_i \approx \theta_i$, and $\cos \theta_i \approx 1$.

3.2. Potential energy

The theorem of potential energy, as stated by Germain and Muller in [15], reads:

For a given problem, among all cinematically admissible-fields (C') the real displacement field is the one that minimizes the potential energy of the system.

The potential energy $V(C')$ of a body, resulting from a cinematically admissible displacement-field is defined by:

$$V(C') = W(C') - \iiint f_k \cdot U_k' dv - \iint T_k \cdot U_k' ds \quad (3)$$

$W(C')$ is the strain energy of the structure, f_k is the component of the external volume force, T_k is the component of the surface force being exerted on the system and $U_k'(M)$ is the component of the admissible displacement of any point M of the system.

It is this property of the real displacement field which will be exploited in the proposed optimization method.

3.3. Relationships between the design variables

The kinematic composition law for the relative motions allowed by each of the joints implies that:

$$\{\mathbf{T}_1(S_1/S_0)\} = \{\mathbf{T}_2(S_1/S_0)\} \quad (4)$$

In equality (4), each kinematic vectorial-set should be reduced to the same point.

The small displacements $\{\mathbf{T}_1(S_1/S_0)\}_{A_1}$ and $\{\mathbf{T}_1(S_1/S_0)\}_{A_2}$ are respectively written as:

$$\{\mathbf{T}_1(S_1/S_0)\}_{A_1} = \begin{Bmatrix} u_1 & \alpha_1 \\ v_1 & \beta_1 \\ w_1 & \gamma_1 \end{Bmatrix} \quad (a) \quad \text{and} \quad \{\mathbf{T}_1(S_1/S_0)\}_{A_2} = \begin{Bmatrix} u_2 & \alpha_2 \\ v_2 & \beta_2 \\ w_2 & \gamma_2 \end{Bmatrix} \quad (b) \quad (5)$$

The development of (4) gives:

$$\mathbf{\Omega}_1(S_1/S_0) = \mathbf{\Omega}_2(S_1/S_0) \quad (6)$$

and

$$\mathbf{V}_{A_2}(S_1/S_0) = \mathbf{V}_{A_1}(S_1/S_0) + \mathbf{O}_2 \mathbf{O}_1 \wedge \mathbf{\Omega}_1(S_1/S_0) \quad (7)$$

In the initial position of mechanism, the points A_1 and A_2 coincide respectively with O_1 and O_2 . The two equalities (6) and (7) give six linear equations linking the design variables.

4. OPTIMIZATION METHOD FOR THE RESEARCH OF RELATIVE PARTS' ARRANGEMENTS

The proposed method computes the values of the small displacements, characterizing the movements authorized by the presence of clearance in the joints, and determines their components (displacements along the three axes and rotations with respect to these axes).

The optimization problem deals with the minimization of the potential energy of the system and accounts for the geometrical, mechanical and technological constraints imposed by the design of the machine. A mathematical optimization-algorithm is used in order to compute the values of the small displacements in the joints which are the design variables of the problem. Mathematically, the optimization problem can be formulated in the form of:

$$\text{Minimize } V(\mathbf{x}) \quad (8a)$$

Subjected to the following optimization constraints:

$$g_j(\mathbf{x}) \leq 0 \quad j = 1, \dots, m \quad (8b)$$

$$h_k(\mathbf{x}) = 0 \quad k = 1, \dots, n \quad (8c)$$

\mathbf{x} is the vector of the design variables which are the components u_i , v_i , w_i , α_i , β_i , and γ_i , of the two vectors $\mathbf{\Omega}_i(S_1/S_0)$ and $\mathbf{V}_{A_i}(S_1/S_0)$ with $i = 1, 2$.

$g_j(\mathbf{x})$ and $h_k(\mathbf{x})$ are respectively the inequality and equality constraints of the problem. In this study, they arise from the geometry of the linkages, the displacement's limits of particular points and from the closing loops' equations (6) and (7).

5. OPTIMIZATION PROCESS

The optimization process can be sketched in the following diagram:

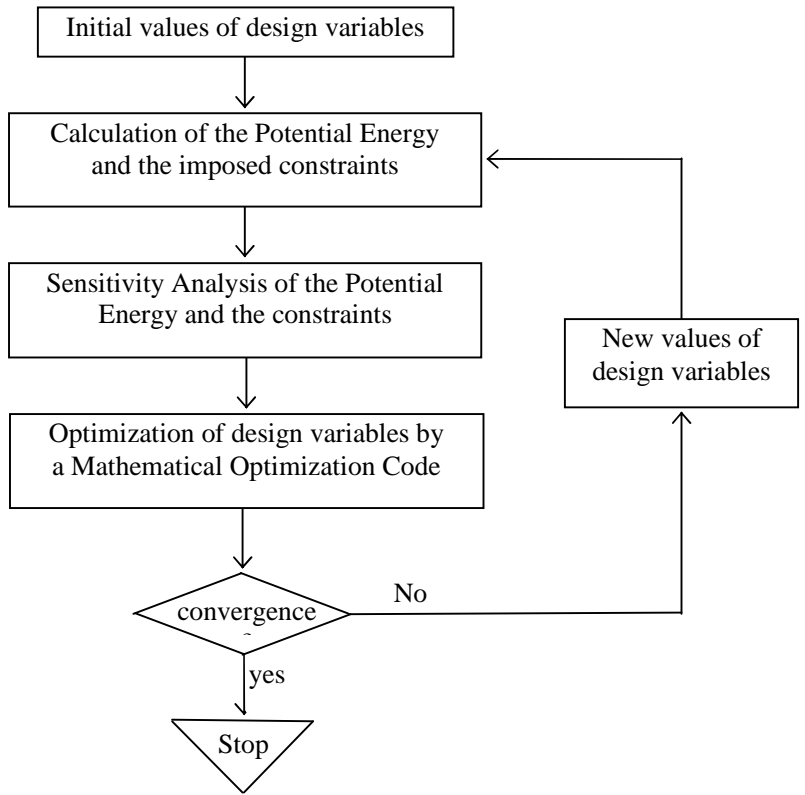


Figure 3. Optimization Algorithm

The purpose of this study is the computation of the equilibrium positions of various elements in spatial mechanisms with parallel joints subjected to mechanical loadings. The values of the design variables being initialized, the initial values of the objective function and the constraints are calculated.

Concerning the search for the optimal solution of the optimization problem, it will be noticed that the majority of optimization methods involve mathematical calculation of the gradients of the objective-function and constraints, by means of the design parameters. This can be achieved by a sensitivity analysis of the objective function and the constraints when the design parameters vary, leading to the convergence of the optimization process towards the optimal solution. The optimization method implemented is the sequential quadratic programming method [16].

The algorithm is based upon an iterative process in which, at each stage, the design parameters take new values, allowing for the convergence towards the optimal solution. In the case of non-convergence, new values are assigned to the design variables and a new iteration is carried out. This process is repeated until convergence is reached.

6. MECHANISMS WITH CLEARANCES IN THE PARALLEL JOINTS

6.1. Mechanism with a spherical joint and a cylindrical joint

The mechanism is composed of two parts, a shaft S_1 and a reference body S_0 linked together by two joints l_1 and l_2 . l_1 is a spherical joint and l_2 is a cylindrical joint. L_2 is the length of the cylindrical joint. J_1 and J_2 are respectively the joint clearances of l_1 and l_2 . A real arrangement of such mechanism can be viewed in Figure 2.

The points A_1 and A_2 lie on the center line of the shaft. They coincide respectively with O and O_2 in the initial position. $OXYZ$ is the global reference frame with its origin O and $O_2X_2Y_2Z_2$ the local reference frame of the cylindrical joint of center O_2 . The scheme of this mechanism is given by figure 4:

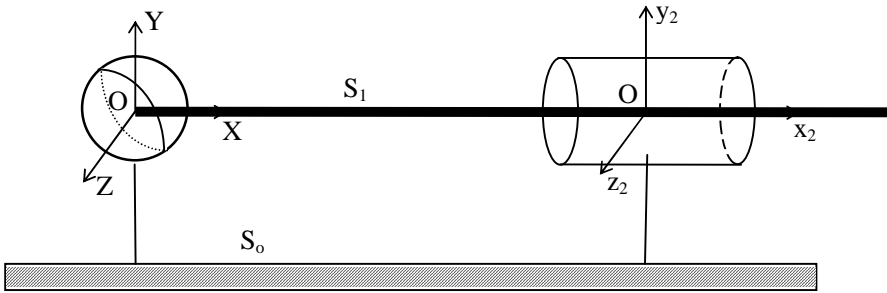


Figure 4. Clearance model of spherical and cylindrical joints

The design variables of the problem are:

- the displacements u_1 , v_1 and w_1 of points A_1 along X , Y and Z axis
- the rotations α_1 , β_1 and γ_1 of the shaft at points A_1 around the X , Y and Z axis
- the displacements u_2 , v_2 and w_2 of points A_2 along X_2 , Y_2 and Z_2 axis
- the rotations α_2 , β_2 and γ_2 of the shaft at points A_2 around the X_2 , Y_2 and Z_2 axis.

6.1.1. Objective-function

A torque C and a force F applied at point B on the shaft are the components of the mechanical loading. The potential energy is expressed as:

$$V(C) = - (\mathbf{F} \cdot \mathbf{U}_B + C \cdot \Theta_B) \quad (9)$$

\mathbf{U}_B and Θ_B , respectively the displacement vector and the rotation vector of point B , are calculate by means of $\{\mathbf{T}_i(S_1/S_0)\}_{A_i}$ in a same manner as equation (7).

6.1.2. Limits of design variables

The values of the design variables are limited by the geometry of the joints. They are characterized by the following inequalities:

a. Spherical joint

$$-\frac{J_1}{2} \leq u_1 \leq \frac{J_1}{2} \quad (\text{a}); \quad -\frac{J_1}{2} \leq v_1 \leq \frac{J_1}{2} \quad (\text{b}); \quad -\frac{J_1}{2} \leq w_1 \leq \frac{J_1}{2} \quad (\text{c}) \quad (10)$$

$$-\infty \leq \alpha_1 \leq \infty \quad (\text{a}); \quad -\infty \leq \beta_1 \leq \infty \quad (\text{b}); \quad -\infty \leq \gamma_1 \leq \infty \quad (\text{c}) \quad (11)$$

b. Cylindrical joint

$$-\infty \leq u_2 \leq \infty \quad (\text{a}); \quad -\frac{J_2}{2} \leq v_2 \leq \frac{J_2}{2} \quad (\text{b}); \quad -\frac{J_2}{2} \leq w_2 \leq \frac{J_2}{2} \quad (\text{c}) \quad (12)$$

$$-\infty \leq \alpha_2 \leq \infty \quad (\text{a}); \quad -\frac{J_2}{L_2} \leq \beta_2 \leq \frac{J_2}{L_2} \quad (\text{b}); \quad -\frac{J_2}{L_2} \leq \gamma_2 \leq \frac{J_2}{L_2} \quad (\text{c}) \quad (13)$$

6.1.3. Linear geometric constraints

That kind of constraints appears when the contacts between the shaft and the joints are accounted for and when closing the kinematic vectors chain.

a. Cylindrical joint

For that joint, in the $O_2x_2y_2$ plane, the displacements along the axis y_2 are limited by upper and lower contacts shaft/cylinder of the points with abscises $L_2/2$ and $-L_2/2$. They are respectively written in explicit form by:

$$v_2 + \gamma_2 \frac{L_2}{2} \quad (14a)$$

$$v_2 - \gamma_2 \frac{L_2}{2} \quad (14b)$$

These displacements should not exceed the boundaries $\left[-\frac{J_2}{2}, \frac{J_2}{2} \right]$, involving the two

following linear inequalities:

$$-\frac{J_2}{2} \leq v_2 + \gamma_2 \frac{L_2}{2} \leq \frac{J_2}{2} \quad (15a)$$

$$-\frac{J_2}{2} \leq v_2 - \gamma_2 \frac{L_2}{2} \leq \frac{J_2}{2} \quad (15b)$$

For the same joint but in the $O_2x_2z_2$ plane, we obtain:

$$-\frac{J_2}{2} \leq w_2 + \beta_2 \frac{L_2}{2} \leq \frac{J_2}{2} \quad (16a)$$

$$-\frac{J_2}{2} \leq w_2 - \beta_2 \frac{L_2}{2} \leq \frac{J_2}{2} \quad (16b)$$

b. Kinematic equation

Now, for each kind of joint, the explicit form of the kinematic closing loop (6) and (7) leads to the six linear independent equations:

$$\begin{Bmatrix} \alpha_1 \\ \beta_1 \\ \gamma_1 \end{Bmatrix} - \begin{Bmatrix} \alpha_2 \\ \beta_2 \\ \gamma_2 \end{Bmatrix} = \begin{Bmatrix} \tau \\ 0 \end{Bmatrix} \quad (17a)$$

$$\begin{Bmatrix} u_2 \\ v_2 \\ w_2 \end{Bmatrix} - \begin{Bmatrix} u_1 \\ v_1 \\ w_1 \end{Bmatrix} - \overrightarrow{O_2 O_1} \Lambda \begin{Bmatrix} \alpha_1 \\ \beta_1 \\ \gamma_1 \end{Bmatrix} = \begin{Bmatrix} \tau \\ 0 \end{Bmatrix} \quad (17b)$$

6.1.4. Non-Linear geometric constraints

These constraints are due to the limited movement of the shaft in the cylindrical or spherical clearance space. It leads to the following quadratic inequalities:

$$0 \leq u_1^2 + v_1^2 + w_1^2 \leq \left(\frac{J_1}{2}\right)^2 \quad (18)$$

$$0 \leq \left(v_2 + \gamma_2 \frac{L_2}{2}\right)^2 + \left(w_2 - \beta_2 \frac{L_2}{2}\right)^2 \leq \left(\frac{J_2}{2}\right)^2 \quad (19)$$

$$0 \leq \left(v_2 - \gamma_2 \frac{L_2}{2}\right)^2 + \left(w_2 + \beta_2 \frac{L_2}{2}\right)^2 \leq \left(\frac{J_2}{2}\right)^2 \quad (20)$$

6.1.5. Shaft loading

The shaft can be loaded in several ways, including forces and torques applied at various points. Three cases of shaft mounting will be studied, each one being subjected two various loading conditions. The numerical applications will allow to validate the formulation.

6.1.6 Spherical and cylindrical joints arrangement

The spherical joint is placed at the origin O and the clearance value J_1 is 0.2mm. The cylindrical joint at the other end has a length $L_2=40$ mm and a clearance value $J_2 = 0.2$ mm. The distance $A_1A_2 = 200$ mm on X axis. In unloaded position, A_1 coincides with O.

6.1.6.1 First loading case

The shaft is loaded at right and out of the cylindrical joint by a force $\mathbf{F} = \begin{Bmatrix} 1\text{N} \\ 1\text{N} \\ 1\text{N} \end{Bmatrix}$. The distance A_2B

will have no influence on the optimal relative position.

The method allows finding the optimal solution of the displacements and rotations of the shaft at points A_1 and A_2 . The numerical results obtained at the end of the optimization process, are reported in the following vectors sets (the first column refers to the displacements (mm) and the second to the rotations of the shaft (rad)):

$$\left\{ \begin{array}{l} \{ {}_1(S_1/S_0) \}_{A_1} \\ \{ {}_2(S_1/S_0) \}_{A_2} \end{array} \right. = \left\{ \begin{array}{l} \left. \begin{array}{l} u_1 = 8.892973 \cdot 10^{-2} \text{ mm} \\ v_1 = -3.233808 \cdot 10^{-2} \text{ mm} \\ w_1 = -3.233806 \cdot 10^{-2} \text{ mm} \end{array} \right\} \begin{array}{l} \alpha_1 = -1.562943 \cdot 10^{-306} \text{ rad} \\ \beta_1 = -4.684034 \cdot 10^{-4} \text{ rad} \\ \gamma_1 = 4.684034 \cdot 10^{-4} \text{ rad} \end{array} \right. \\ \left. \begin{array}{l} u_2 = 8.892973 \cdot 10^{-2} \text{ mm} \\ v_2 = 6.134259 \cdot 10^{-2} \text{ mm} \\ w_2 = 6.134262 \cdot 10^{-2} \text{ mm} \end{array} \right\} \begin{array}{l} \alpha_2 = -1.524142 \cdot 10^{-306} \text{ rad} \\ \beta_2 = -4.684034 \cdot 10^{-4} \text{ rad} \\ \gamma_2 = 4.684034 \cdot 10^{-4} \text{ rad} \end{array} \right.$$

From these values, it follows that the displacements of the center A_1 of the spherical joint satisfy the relation $\sqrt{u_1^2 + v_1^2 + w_1^2} = \frac{J_1}{2} = 0.1 \text{ mm}$. Thus, the final position of point A_1 is located on the sphere with a radius equal to the clearance value.

Concerning the point A_2 , it moves along the three axes x_2 , y_2 and z_2 with rotations β_2 and γ_2 between the boundaries $-J_2/L_2$ and J_2/L_2 . The rotation α_2 is negligible. In addition, the linear constraints given in the relations (15) and (16) respect their boundaries $-J_2/2$ and $J_2/2$:

$$v_2 + \gamma_2 \frac{L_2}{2} = 7.071066 \cdot 10^{-2} \text{ mm}, \quad v_2 - \gamma_2 \frac{L_2}{2} = 5.197453 \cdot 10^{-2} \text{ mm},$$

$$w_2 + \beta_2 \frac{L}{2} = 5.197456 \cdot 10^{-2} \text{ mm}, \quad w_2 - \beta_2 \frac{L}{2} = 7.071069 \cdot 10^{-2} \text{ mm}.$$

Furthermore, since the value of nonlinear constraint (19) is equal to the upper boundary: $\left(v_2 + \gamma_2 \frac{L_2}{2} \right)^2 + \left(w_2 - \beta_2 \frac{L_2}{2} \right)^2 = \left(\frac{J_2}{2} \right)^2 = 0.01 \text{ mm}^2$, then the contact between the shaft and the right side of the cylindrical joint is assured. But the nonlinear constraint (20) does not achieve their upper bound: $\left(v_2 - \gamma_2 \frac{L_2}{2} \right)^2 + \left(w_2 + \beta_2 \frac{L_2}{2} \right)^2 = 5.402706 \cdot 10^{-3} \text{ mm}^2 < \left(\frac{J_2}{2} \right)^2$, so the left side of the cylindrical joint has no contact with the shaft as indicated in figure 5.

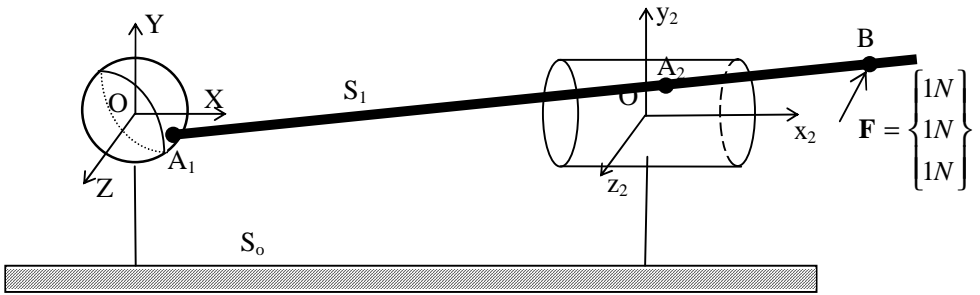


Figure 5. Displacement of the shaft after loading

Now if the force values are different from 1N, it will not be obvious to give an accurate prediction of the exact position of the parts. A purely geometrical calculation is no more possible for the

computation of the relative displacements values because the components of the force will influence the result.

In the case where spherical joint has a clearance very large compared to that of cylindrical joint ($J_1 = 3$ mm, $J_2 = 0.1$ mm and $L_2 = 40$ mm), the optimization algorithm converges to optimal values of displacements and rotations of shaft in the points A_1 and A_2 given respectively in $\{\mathcal{T}_1(S_1/S_0)\}_{A_1}$ and $\{\mathcal{T}_2(S_1/S_0)\}_{A_2}$:

$$\{\mathcal{T}_1(S_1/S_0)\}_{A_1} = \begin{Bmatrix} 1.41421356 \text{ mm} & -5.25281282 \cdot 10^{-16} \text{ rad} \\ -0.35355338 \text{ mm} & -1.76776695 \cdot 10^{-3} \text{ rad} \\ -0.35355339 \text{ mm} & 1.76776694 \cdot 10^{-3} \text{ rad} \end{Bmatrix}$$

$$\{\mathcal{T}_2(S_1/S_0)\}_{A_2} = \begin{Bmatrix} 1.41421356 \text{ mm} & -5.25281282 \cdot 10^{-16} \text{ rad} \\ -3.20688982 \cdot 10^{-10} \text{ mm} & -1.76776695 \cdot 10^{-3} \text{ rad} \\ 3.20706891 \cdot 10^{-10} \text{ mm} & 1.76776694 \cdot 10^{-3} \text{ rad} \end{Bmatrix}$$

The nonlinear constraints have the following values:

$$u_1^2 + v_1^2 + w_1^2 = 2.250000 \text{ mm}^2 = \left(\frac{J_1}{2}\right)^2$$

$$\left(v_2 + \gamma_2 \frac{L_2}{2}\right)^2 + \left(w_2 - \beta_2 \frac{L_2}{2}\right)^2 = 2.50000 \cdot 10^{-3} \text{ mm}^2 = \left(\frac{J_2}{2}\right)^2$$

$$\left(v_2 - \gamma_2 \frac{L_2}{2}\right)^2 + \left(w_2 + \beta_2 \frac{L_2}{2}\right)^2 = 2.50000 \cdot 10^{-3} \text{ mm}^2 = \left(\frac{J_2}{2}\right)^2$$

Since the nonlinear constraints reach their upper boundaries, the point A_1 is located on the sphere of the spherical joint and there are two contacts between the shaft and the cylindrical joint.

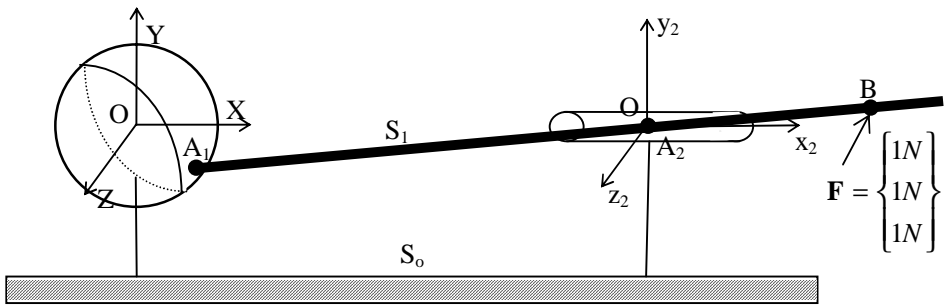


Figure 6. Contact of the shaft with the joints

6.1.6.2 Second loading case

The dimensions and clearances of the first case are unchanged ($J_1 = 0.2 \text{ mm}$, $J_2 = 0.2 \text{ mm}$, $L_2 = 40 \text{ mm}$ and $A_1 A_2 = 200 \text{ mm}$) but the shaft is loaded at its middle point B by a force $\mathbf{F} = \begin{Bmatrix} 0 \text{ N} \\ 1 \text{ N} \\ 1 \text{ N} \end{Bmatrix}$.

After computations and convergence of the algorithm, the optimum values are reported below:

$$\left\{ \begin{matrix} {}_1(S_1/S_0) \end{matrix} \right\}_{A_1} = \begin{Bmatrix} 9.09985988 \cdot 10^{-259} \text{ mm} & -1.59740463 \cdot 10^{-274} \text{ rad} \\ 7.07106780 \cdot 10^{-2} \text{ mm} & 1.65058153 \cdot 10^{-13} \text{ rad} \\ 7.07106781 \cdot 10^{-2} \text{ mm} & 1.65050781 \cdot 10^{-13} \text{ rad} \end{Bmatrix}$$

$$\left\{ \begin{matrix} {}_2(S_1/S_0) \end{matrix} \right\}_{A_2} = \begin{Bmatrix} 9.09985988 \cdot 10^{-259} \text{ mm} & -1.59740463 \cdot 10^{-274} \text{ rad} \\ 7.07106781 \cdot 10^{-2} \text{ mm} & 1.65058234 \cdot 10^{-13} \text{ rad} \\ 7.07106781 \cdot 10^{-2} \text{ mm} & 1.65051596 \cdot 10^{-13} \text{ rad} \end{Bmatrix}$$

Results show that the shaft moves only in the plane OYZ without any rotation. The schematic view of the mechanism is presented in figure 7.

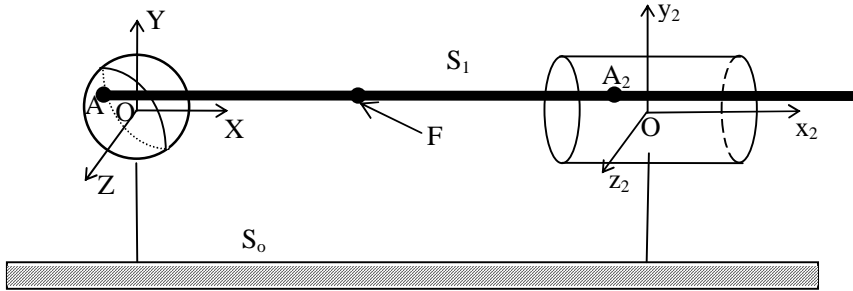


Figure 7. Shaft position after loading

The optimal values of design variables show that the shaft moves in a parallel direction to the x axis without moving along this axis. Since the clearance values of joints are equal, then there is no rotation of shaft. The final position of point A_1 is located on the sphere considering that $\sqrt{7.071^2 + 7.071^2} = 10 = \frac{J_1}{2}$. The final position of point A_2 lies on the circle with a radius $\frac{J_2}{2}$ because $\sqrt{u_2^2 + v_2^2 + w_2^2} = \frac{J_2}{2}$. Since the clearances in two joints are equal and the load is parallel to the plane OYZ, $\left\{ \begin{matrix} {}_1(S_1/S_0) \end{matrix} \right\}_{A_1}$ and $\left\{ \begin{matrix} {}_2(S_1/S_0) \end{matrix} \right\}_{A_2}$ are identical.

If the clearances in two joints are different, the two following cases are presented: $J_1 > J_2$ and $J_1 < J_2$. The other dimensions and the load case are unchanged.

a- Case 1: $J_1 > J_2$

The clearance in spherical joint is modified from 0.2mm to 0.3mm. The algorithm converges to the following optimum values:

$$\left\{ \begin{array}{l} \{ {}_1(S_1/S_0) \}_{A_1} \\ \{ {}_2(S_1/S_0) \}_{A_2} \end{array} \right\} = \left\{ \begin{array}{ll} \left. \begin{array}{l} -5.40044426 \cdot 10^{-9} \text{ mm} \quad -1.25554283 \cdot 10^{-15} \text{ rad} \\ 0.10606604 \text{ mm} \quad 1.96418180 \cdot 10^{-4} \text{ rad} \\ 0.10606598 \text{ mm} \quad -1.96418919 \cdot 10^{-4} \text{ rad} \end{array} \right\} \\ \left. \begin{array}{l} -5.40044426 \cdot 10^{-9} \text{ mm} \quad -1.25554283 \cdot 10^{-15} \text{ rad} \\ 6.67822643 \cdot 10^{-2} \text{ mm} \quad 1.96418180 \cdot 10^{-4} \text{ rad} \\ 6.67823498 \cdot 10^{-2} \text{ mm} \quad -1.96418919 \cdot 10^{-4} \text{ rad} \end{array} \right\} \end{array} \right.$$

Since $J_1 > J_2$, the optimal values of displacements of A_1 are greater than those of A_2 and there is only a rotation of the shaft relative to the two axes y_2 and z_2 .

The point A_1 is located on the sphere of the spherical joint because $\sqrt{u_1^2 + v_1^2 + w_1^2} = \frac{J_1}{2}$. In addition, $\left(v_2 + \gamma_2 \frac{L_2}{2} \right)^2 + \left(w_2 - \beta_2 \frac{L_2}{2} \right)^2 = 7,901235 \cdot 10^{-3} \text{ mm}^2 < \left(\frac{J_2}{2} \right)^2 = 0.01 \text{ mm}^2$ and $\left(v_2 - \gamma_2 \frac{L_2}{2} \right)^2 + \left(w_2 + \beta_2 \frac{L_2}{2} \right)^2 = \left(\frac{J_2}{2} \right)^2 = 0.01 \text{ mm}^2$. This shows that there is only one contact between the shaft and the left side of the second joint.

b-Case 2: $J_1 < J_2$

In this case, the clearance of the spherical joint is equal to 0.1mm. After computations and convergence of the algorithm, the numerical values which have been obtained, are reported in the kinematic vectorial-sets:

$$\left\{ \begin{array}{l} \{ {}_1(S_1/S_0) \}_{A_1} \\ \{ {}_2(S_1/S_0) \}_{A_2} \end{array} \right\} = \left\{ \begin{array}{ll} \left. \begin{array}{l} -3.56393699 \cdot 10^{-14} \text{ mm} \quad -1.67486499 \cdot 10^{-17} \text{ rad} \\ 3.53553390 \cdot 10^{-2} \text{ mm} \quad -1.60706086 \cdot 10^{-4} \text{ rad} \\ 3.53553390 \cdot 10^{-2} \text{ mm} \quad 1.60706086 \cdot 10^{-4} \text{ rad} \end{array} \right\} \\ \left. \begin{array}{l} -3.56393699 \cdot 10^{-14} \text{ mm} \quad -1.67486499 \cdot 10^{-17} \text{ rad} \\ 6.74965563 \cdot 10^{-2} \text{ mm} \quad -1.60706086 \cdot 10^{-4} \text{ rad} \\ 6.74965563 \cdot 10^{-2} \text{ mm} \quad 1.60706086 \cdot 10^{-4} \text{ rad} \end{array} \right\} \end{array} \right.$$

The optimal values of displacements of A_1 are smaller than those of A_2 and there are only rotations of the shaft relative to the two axis y_2 and z_2 .

Since $u_1^2 + v_1^2 + w_1^2 = \left(\frac{J_1}{2} \right)^2 = 2.50000 \cdot 10^{-3} \text{ mm}^2$,

$\left(v_2 + \gamma_2 \frac{L_2}{2} \right)^2 + \left(w_2 - \beta_2 \frac{L_2}{2} \right)^2 = \left(\frac{J_2}{2} \right)^2 = 1.000 \cdot 10^{-2} \text{ mm}^2$ and

$\left(v_2 - \gamma_2 \frac{L_2}{2}\right)^2 + \left(w_2 + \beta_2 \frac{L_2}{2}\right)^2 = 8.264463 \cdot 10^{-3} \text{ mm}^2 \leq \left(\frac{J_2}{2}\right)^2$, the conclusions obtained, for this case, are:

- The point A_1 is located on the sphere of the spherical joint.
- There is only one contact between the shaft and the right side of cylindrical joint.

The effectiveness of the method is thus verified.

6.2. Mechanism with two spherical joints

The mechanism has two parts, a shaft S_1 and a reference body S_0 linked together by two spherical joints. A real arrangement of such mechanism can be viewed in Figure 8:

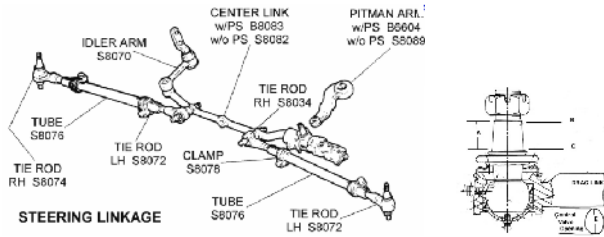


Figure 8. Rod with two spherical joints

In the model, the points A_1 and A_2 at the ends of the shaft are the centers of the spheres on the shaft. They coincide respectively with O and O_2 in the initial position. $OXYZ$ is the global reference frame with its origin O and $O_2X_2Y_2Z_2$ (the local reference frame of the second spherical joint of center O_2). The scheme of this mechanism is given by Figure 9:

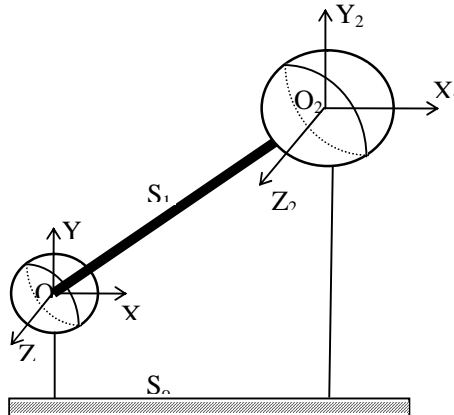


Figure 9. Clearance model of mechanism with two spherical joints

The components of the displacements of points A_1 and A_2 and the rotation of the shaft in the S_0 frame are the design variables. As in the preceding example, the optimization problem is carried out in several cases of shaft loading.

As in the preceding example, an optimization problem is raised allowing the evaluation of the design variables. Several cases of loading will be now considered.

6.2.1. First case of two spherical joints

For the numerical study, the clearance values are chosen to be 0,3 mm in the first joint and 0,6 mm in the second joint.

The center O_2 of the second sphere has as Cartesian coordinates $\mathbf{OO}_2 = \begin{Bmatrix} 200 \\ 400 \\ 600 \end{Bmatrix} \text{ mm}$.

The shaft is loaded at its middle point B by a force $\mathbf{F} = \begin{Bmatrix} 1\text{N} \\ 1\text{N} \\ 1\text{N} \end{Bmatrix}$.

At the end of the optimization process, the optimum values of displacements and rotations are reported below:

$$\left\{ \begin{matrix} 1(S_1/S_0) \end{matrix} \right\}_{A_1} = \begin{Bmatrix} 6.84574801 \cdot 10^{-2} \text{ mm} & -1.24552440 \cdot 10^{-4} \text{ rad} \\ 8.54799757 \cdot 10^{-2} \text{ mm} & 2.49104927 \cdot 10^{-4} \text{ rad} \\ 0.102502425 \text{ mm} & -1.24552477 \cdot 10^{-4} \text{ rad} \end{Bmatrix}$$

$$\left\{ \begin{matrix} 2(S_1/S_0) \end{matrix} \right\}_{A_2} = \begin{Bmatrix} 0.267741427 \text{ mm} & -1.24552440 \cdot 10^{-4} \text{ rad} \\ 0.135300944 \text{ mm} & 2.49104927 \cdot 10^{-4} \text{ rad} \\ 2.86046329 \cdot 10^{-3} \text{ mm} & -1.24552477 \cdot 10^{-4} \text{ rad} \end{Bmatrix}$$

From these values, it follows that the displacements of each center of the spherical joints satisfy the relation $\sqrt{u_i^2 + v_i^2 + w_i^2} = \frac{J_i}{2}$ ($i = 1, 2$). Thus, the final positions of the points A_1 and A_2 are located on the two spheres of clearance as shown in Figure 10:

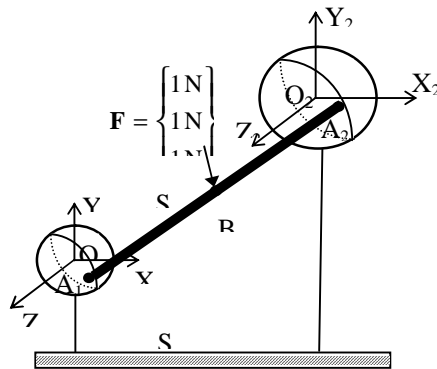


Figure 10. Displacements of the shaft after loading

6.2.2. Second case of two spherical joints

We suppose in this section that the two joints have the same clearance value equal to 0.3 mm. The other dimensions and the load case are unchanged.

$$\{ {}_1(S_1/S_0) \}_{A_1} = \begin{Bmatrix} 8.66025403 \cdot 10^{-2} \text{ mm} & 1.06758281 \cdot 10^{-15} \text{ rad} \\ 8.66025403 \cdot 10^{-2} \text{ mm} & 2.13479904 \cdot 10^{-15} \text{ rad} \\ 8.66025403 \cdot 10^{-2} \text{ mm} & 3.20236638 \cdot 10^{-15} \text{ rad} \end{Bmatrix}$$

$$\{ {}_2(S_1/S_0) \}_{A_2} = \begin{Bmatrix} 8.66025403 \cdot 10^{-2} \text{ mm} & 1.06757756 \cdot 10^{-15} \text{ rad} \\ 8.66025403 \cdot 10^{-2} \text{ mm} & 2.13481067 \cdot 10^{-15} \text{ rad} \\ 8.66025403 \cdot 10^{-2} \text{ mm} & 3.20236229 \cdot 10^{-15} \text{ rad} \end{Bmatrix}$$

The results show that $\{ \boldsymbol{\tau}_1(S_1/S_0) \}_{A_1}$ has the same value of $\{ \boldsymbol{\tau}_2(S_1/S_0) \}_{A_2}$. In addition, there are no rotation (numerical values are negligible) of the shaft which is logical.

After computations and convergence of the algorithm, the schematic view of the mechanism is presented in figure 11.

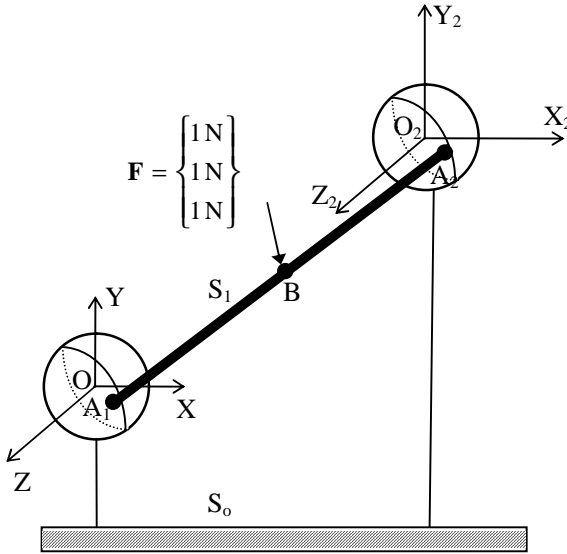


Figure 11. Shaft position after loading

Since $\sqrt{u_i^2 + v_i^2 + w_i^2} = \frac{J_i}{2}$, the final positions of the points A_1 and A_2 are located on the spheres defined by the clearance values J_1 and J_2 .

The effectiveness of the method is thus established knowing that the computation of the optimization algorithms must be reliable.

6.3. Mechanism with two cylindrical joints

The mechanism has two parts, a shaft S_1 and a reference body S_0 linked together by two cylindrical joints l_1 and l_2 .

A real arrangement of such mechanism can be viewed in Figure 12.

According to the optimal values, the nonlinear constraints of problem are limited as follows:

$$0 \leq \left(v_1 + \gamma_1 \frac{L_1}{2} \right)^2 + \left(w_1 - \beta_1 \frac{L_1}{2} \right)^2 = 1.000000 \cdot 10^{-2} \text{ mm}^2 \leq \left(\frac{J_1}{2} \right)^2 = 1.000000 \cdot 10^{-2} \text{ mm}^2$$

$$0 \leq \left(v_1 - \gamma_1 \frac{L_1}{2} \right)^2 + \left(w_1 + \beta_1 \frac{L_1}{2} \right)^2 = 1.000000 \cdot 10^{-2} \text{ mm}^2 \leq \left(\frac{J_1}{2} \right)^2 = 1.000000 \cdot 10^{-2} \text{ mm}^2$$

$$0 \leq \left(v_2 + \gamma_2 \frac{L_2}{2} \right)^2 + \left(w_2 - \beta_2 \frac{L_2}{2} \right)^2 = 1.000000 \cdot 10^{-2} \text{ mm}^2 \leq \left(\frac{J_2}{2} \right)^2 = 1.000000 \cdot 10^{-2} \text{ mm}^2$$

$$0 \leq \left(v_2 - \gamma_2 \frac{L_2}{2} \right)^2 + \left(w_2 + \beta_2 \frac{L_2}{2} \right)^2 = 1.000000 \cdot 10^{-2} \text{ mm}^2 \leq \left(\frac{J_2}{2} \right)^2 = 1.000000 \cdot 10^{-2} \text{ mm}^2$$

Since $\sqrt{v_i^2 + w_i^2} = \frac{J_i}{2}$, the final positions of the points A_1 and A_2 are located on the circles defined by the clearance values J_1 and J_2 . The results show that the shaft moves only along the Y and Z axis. In addition, there is no rotation of the shaft.

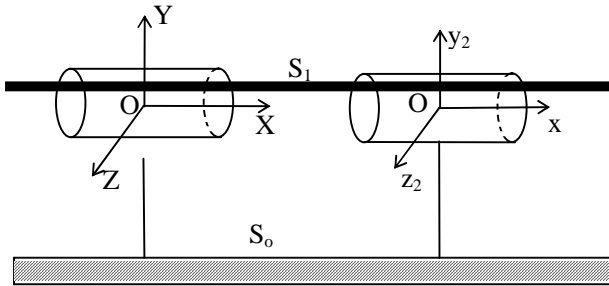


Figure 14. Displacement of the shaft after loading

6.3.2. Second case of two cylindrical joints

A transverse torque $C_z = 1 \text{ Nm}$ is applied in B to the right of the joint l_2 , along the X axis. In this section, the value of the first joint clearance is four times that of the second connection ($J_1 = 0,4 \text{ mm}$ and $J_2 = 0,1 \text{ mm}$) but the length of the second joint is greater than that of the first ($L_1 = 40 \text{ mm}$ and $L_2 = 60 \text{ mm}$). The other dimensions and load cases are similar to the previous case.

After computations and convergence of the algorithm, the numerical values are reported in the kinematic vectorial-sets:

$$\left\{ {}_1(S_1/S_0) \right\}_{A_1} = \left\{ \begin{array}{ll} -3.20084144 \cdot 10^{-308} \text{ mm} & 1.82228772 \cdot 10^{-308} \text{ rad} \\ -0.166666666 \text{ mm} & 5.53813565 \cdot 10^{-8} \text{ rad} \\ 5.96041716 \cdot 10^{-5} \text{ mm} & 1.66666666 \cdot 10^{-3} \text{ rad} \end{array} \right\}$$

$$\left\{ {}_2(S_1/S_0) \right\}_{A_2} = \begin{Bmatrix} -3.35496565 \cdot 10^{-308} \text{ mm} & 3.13762951 \cdot 10^{-308} \text{ rad} \\ -8.13538007 \cdot 10^{-19} \text{ mm} & 5.53813565 \cdot 10^{-8} \text{ rad} \\ 5.40660360 \cdot 10^{-5} \text{ mm} & 1.66666666 \cdot 10^{-3} \text{ rad} \end{Bmatrix}$$

From the numerical values, the equilibrium position of shaft is given on the following figure 16:

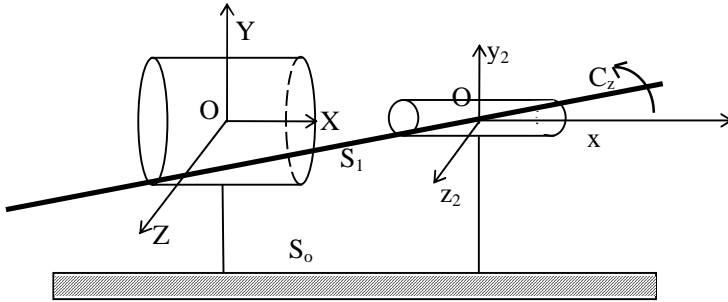


Figure 15. Displacements of the shaft after loading

This equilibrium position of the shaft is normal because $\frac{J_2}{L_2} = \frac{J_1 + J_2}{L_1 + L_2 + 2O_1O_2}$. This causes rotations with respect to the Z axis equal to: $\gamma_1 = \gamma_2 = \frac{J_2}{L_2} = \frac{J_1 + J_2}{L_1 + L_2 + 2O_1O_2} = 1.666 \cdot 10^{-3} \text{ rad}$.

Only in this case, there are three contacts between the shaft and the two mechanism joints.

In the following, consider the case where $\frac{J_2}{L_2} < \frac{J_1 + J_2}{L_1 + L_2 + 2O_1O_2}$. The clearance J_1 is increased to the value 0.5 mm. Results show that the displacement v_1 and the rotations γ_1 et γ_2 are similar to the previous case. Other unknowns are also negligible.

The values of nonlinear constraints are similar to those of the previous result. The difference is in the upper boundaries of the constraints concerning the left joint. They are varied from $4 \cdot 10^{-2} \text{ mm}^2$ to $6.25 \cdot 10^{-2} \text{ mm}^2$. In this case, these constraints are lower than the upper boundaries.

It is found that the shaft is in contact with the two circles of the second joint boundary while there is no contact with the first joint as presented in the following figure:

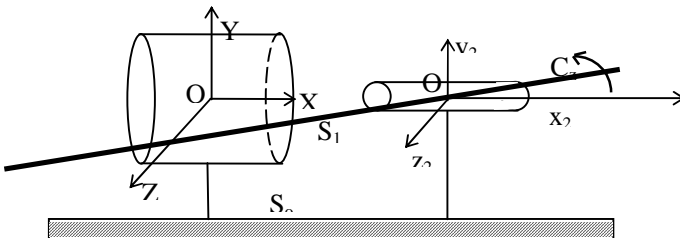


Figure 16. Displacements of the shaft after loading

7. CONCLUSION

The search of maximum accuracy for optimum machine performances requires the control of the clearance in the mechanical joints between the different components. This could be obtained by determining the small variations of the parts position subjected to mechanical loadings. Optimization technique allows the development of new tools for engineers and designers in order to predict and quantify the effects of the joints' clearance on the geometrical performances of mechanisms. It has been shown that without a general method, it's difficult, even impossible, to manually compute the small relative-displacements values induced by the joints' clearance.

This paper has presented a comprehensive method for modeling and analyzing the position of bodies in three-dimensional mechanical assemblies in the case of mechanism with clearance in the parallel joints.

Therefore, we propose to study and calculate the relative positions of mechanical elements using the minimization of the total potential energy in parallel mechanism.

The deformations of the bodies are not considered in the actual formulation, but it can be easily accounted for, by calculating the strain energy of each structural element.

The solution of this problem must use a mathematical optimization-algorithm computing the values of the small displacements in the joints, which are the design variables. Several examples have been presented to evaluate the effectiveness of the formulation. The results obtained from several simulations show the effectiveness of the method.

REFERENCES

- [1] Potiron A., Dal Santo P., Younes M., "Étude bidimensionnelle du positionnement relatif des éléments de mécanismes avec jeu dans les liaisons par une méthode d'optimisation", *Mécanique & Industries* vol. 4, pp. 229–238, 2003.
- [2] Funabashi H., Ogawa K. and Horie M., "A Dynamic Analysis of Mechanisms with Clearance", *Bulletin of the JSME*, vol. 21, N °161: 1652-1659, November 1978.
- [3] Giordano, M., and collective, "Modèle de détermination des tolérances géométriques", In: Tollenaere, M., *Conception de produits mécaniques*. Chapter 13, HERMES Paris, 1998.
- [4] Giordano, M. and Duret, D., "Clearance Space and Deviation Space. Application to three-dimensional chain of dimensions and positions", In "Proc. of the 3rd CIRP Seminars one Tolerancing Computer-Aided", Eyrolles, Cachan, France, 1993.
- [5] Gao J., Chase K. W. and Magleby S. P., "General 3-D Tolerance Analysis of Mechanical Assemblies with Small Kinematic Adjustments", *IIE Transactions*, 30: 367-377, 1998.
- [6] Chase, K. W., Gao, J., and Magleby, S. P., "General 2-D Tolerance Analysis of Mechanical Assemblies with Small Kinematic Adjustments", *J. of Design and Manufacture*, 5: 263-274, 1995.
- [7] Chase, K. W., and Parkinson, A. R., "A Survey of Research in the Application of Tolerance Analysis to the Design of Mechanical Assemblies", *Research in Engineering Design*, 3: 23-37, 1991.
- [8] Flores P. and Ambrosio J., "Revolute joints with clearance in multibody systems", *Computers and Structures*, vol. 82, pp.1359–1369, 2004.
- [9] Turner M., Perkins D., Murray A., Larochelle P., "Systematic Process for Constructing Spherical Four-Bar Mechanisms", *Proceedings of IMECE2005, 2005 ASME International Mechanical Engineering Congress and Exposition, November 5-11, Orlando, Florida USA, 2005.*
- [10] Liu C., Zhang K., Yang L., "The compliance contact model of cylindrical joints with clearances", *Acta Mechanica Sinica*, vol. 21, issue 5, pp. 451-458, 2005.
- [11] Thomas U., Maciuszek I., Wahl F. M., "A Unified Notation for Serial, Parallel, and Hybrid Kinematic Structures", *Proceedings of the 2002 IEEE, International Conference on Robotics & Automation, Washington, DC, May 2002.*

- [12] Fischer I. S., "Numerical analysis of displacements in spatial mechanisms with ball joints", *Mechanism and Machine Theory*, Volume 35, Issue 11, Pages 1623–1640, 2000.
- [13] Hsieh J.-F., "Numerical Analysis of Displacements in Spatial Mechanisms with Spherical Joints utilizing an extended D-H notation, *Transactions of the Canadian Society for Mechanical Engineering*, Vol. 34, No. 3–4, pp. 417-431, 2010.
- [14] Erkaya S., Uzmay I., "Investigation on effect of joint clearance on dynamics of four-bar mechanism", *Nonlinear Dynamics*, Volume 58, Issue 1-2, pp 179-198, 2009.
- [15] Germain P. and Muller P., "Introduction à la mécanique des milieux continus", Masson, Ed. 1980.
- [16] Vanderplaats G. N., "Numerical optimization techniques for engineering design with applications", Mc Graw-Hill Book company, 1984.